RSC Advances

PAPER

View Article Online
View Journal | View Issue

Cite this: *RSC Adv.*, 2024, **14**, 5417

Photoinduced deformation behavior of poly(aryl ether)s with different azobenzene groups in the side chain†

Jie Yi,[a] Yajing Yang,[b] Xi-ming Song *[a] and Yuxuan Zhang *[a]

Azobenzene-containing poly(aryl ether)s are a potential type of photoinduced deformable high-performance polymer. However, research on photoinduced deformation of azobenzene-containing poly(aryl ether)s focuses mainly on poly(aryl ether)s containing azobenzene groups in the main chain. In this paper, the photoinduced deformation of poly(aryl ether)s containing azobenzene groups in the side chain was studied for the first time. Two novel poly(aryl ether)s containing azobenzene groups in the side chain were synthesized, and their photoinduced isomerization behavior and photoinduced deformation behavior were studied. It could be seen that the match of the excitation luminescence to the maximum absorption peak of the azobenzene groups was more compatible, and the photoinduced motion of the polymers was faster. In addition, poly(aryl ether)s containing azobenzene groups in the side chain showed highly stable photoinduced deformation. The results of this work will be helpful for designing polymers which could be controlled by lasers of different wavelengths.

Received 19th December 2023
Accepted 22nd January 2024

DOI: 10.1039/d3ra08664j

rsc.li/rsc-advances

1. Introduction

Shape changes in polymer materials can be achieved under different stimuli,[1–3] such as light,[4] heat,[5] electricity,[6] magnetism,[7] pH,[8] or ionic strength.[9] Photoresponsive polymers[10,11] refer to macromolecules that undergo physical or chemical changes when exposed to specific wavelengths of light. Such changes in intramolecular or intermolecular motion can be translated into large-scale motion of chain segments or even macroscopic motion of materials.[12,13] Photoresponsive polymers usually contain photosensitive groups, which experience certain chemical or physical reactions after absorbing specific wavelengths of light, resulting in a series of structural and performance changes, thereby exhibiting specific functions.

As a type of photoresponsive polymer, azobenzene-containing polymers (azo-polymers) have been widely studied due to the reversible photoisomerization and photoinduced anisotropy of azobenzene groups. Azo-polymers show a variety of photoresponsive variations with potential applications in optical data storage, photoresponsive materials, and nonlinear optical materials.[14–18] In recent years, the photoinduced deformation behavior of azo-polymers has become a research hotspot.[19,20] The photoinduced isomerization behavior of azobenzene groups can lead to changes in the geometric structure of azobenzene groups. Thus, at the macroscopic level, azo-polymers could exhibit photoinduced deformation.[21,22] Photomechanical effects of azo-polymers are generally studied using film cantilevers of the azo-polymers. The excitation laser is attenuated throughout the thickness of the films, which creates a strain gradient on the film cantilevers.[23]

Among photodeformable azo-polymers, azobenzene-containing liquid crystalline polymers have been widely studied.[24–26] However, azobenzene-containing liquid crystalline polymers have the disadvantage of poor thermal stability. Photoinduced deformable high-performance azobenzene-containing polymers have research value due to their excellent thermal stability and mechanical properties. Photoinduced deformable high-performance azobenzene-containing polymers are mainly polyimides, polyamides, and poly(aryl ether)s.[27–29] Compared to the other two kinds of polymer, azobenzene-containing poly (aryl ether)s show greater potential for application due to their faster photoinduced deformable behavior.

Research on the photoinduced deformation of azobenzene-containing poly(aryl ether)s focuses mainly on poly(aryl ether)s containing azobenzene groups in the main chain.[30–32] It has been reported that azopolyimides containing azobenzene groups in the side chain could exhibit photoinduced deformation behavior and show good stability of photoinduced deformation.[33] Poly(aryl ether)s containing azobenzene groups in the side chain have received a lot of attention due to their potential applications in optical storage and fluorescence micropatterns.[34,35] However, there has been no research on the photoinduced deformation behavior of poly(aryl ether)s

[a]College of Chemistry, Liaoning University, Shenyang, 110036, China. E-mail: zhangyuxuan@lnu.edu.cn
[b]School of Pharmaceutical Engineering, Shenyang Pharmaceutical University, Shenyang 110016, China

† Electronic supplementary information (ESI) available. See DOI: https://doi.org/10.1039/d3ra08664j

containing azobenzene groups in the side chain. In this work, the photoinduced deformation of poly(aryl ether)s containing azobenzene groups in the side chain was studied. Two novel poly(aryl ether)s containing azobenzene groups in the side chain were synthesized, and their photoresponsive properties under different excitation luminescence were studied.

2. Materials

2.1. Materials

4-Bromoaniline, 1,4-benzoquinone, phenol, 4-aminophenyl acetylene, 4,4′-dimethylaminophenyl acetylene, bis(triphenylphosphine)dichloropalladium, sodium bicarbonate, sodium acetate, *p*-anisidine, triethylamine, 2,2,6,6-tetramethylheptane-3,5-dione, and 4,4′-dichlorodiphenyl sulfone were purchased from Adamas-Beta. K_2CO_3, CuI, Cs_2CO_3, CuCl, iron powder, and zinc powder were obtained from Aladdin.

2.2. Measurements

^{1}H NMR spectra were obtained using a Mercury-300 spectrometer in DMSO-d_6 for all compounds using TMS as an internal standard. Gel permeation chromatography (GPC) was carried out using a Waters 2414 instrument. UV-visible absorption spectra were recorded with a PerkinElmer Lambda 35 UV-vis spectrophotometer. Glass transition temperatures (T_{gs}) were determined with a DSC (Netzsch 200 F3) instrument at a heating rate of 10 °C min^{-1} under nitrogen from 0 °C to 800 °C. The reported T_g value was recorded from the second scan after the sample had first been heated and then quenched. Thermogravimetric analysis was performed with a TGA analyzer (Netzsch TG 209 F3) at a heating rate of 10 °C min^{-1} under a nitrogen atmosphere from 0 °C to 400 °C. 450 nm/532 nm/660 nm LED and 445 nm/532 nm/660 nm laser light sources were used for the photoinduced isomerization testing and photoinduced deformation testing.

2.3. Synthesis

2.3.1. Synthesis of 2-(4′-bromophenyl) hydroquinone (Scheme 1). The synthesis of 2-(4′-bromophenyl) hydroquinone was based on the literature.[35] An aqueous solution (3 mL) of sodium nitrite (1.72 g, 0.025 mol) was added dropwise to a 10 mL aqueous solution of 4-bromoaniline (4.31 g, 0.025 mol) acidified by 6 mol L^{-1} hydrochloric acid (17 mL) at 0–5 °C. Separately, 1,4-benzoquinone (2.68 g, 0.025 mol) and sodium bicarbonate (2.3 g) were dissolved in 100 mL of water and cooled to 0 °C. Then, the diazotized solution was added slowly into the alkaline solution of phenol with continuous stirring in an ice bath. After the addition was complete, stirring was continued for 4 h. The precipitate was filtered, washed with water until the pH of the filtrate was neutral, and dried by vacuum to obtain a yellow solid. 2.0 g of zinc powder and 3 mL of anhydrous ethanol were added to a 30 mL aqueous solution of the above product (2.70 g). The solution was heated to reflux, 7 mL of 6 mol L^{-1} hydrochloric acid was added dropwise, and reflux was continued for 3 hours. The product was filtered while it was still hot. The filtrate was rotated to obtain a gray solid. The crude product was recrystallized from hot deionized water to generate white rod-shaped crystals (0.52 g, 20.0%). ^{1}H NMR (DMSO-d_6, ppm): H_4: 8.89 (s, 1H), H_1: 8.81 (s, 1H), H_7: 7.56 (d, 2H), H_6: 7.46 (d, 2H), H_5: 6.75 (d, 1H), H_3: 6.65 (s, 1H), H_2: 6.59 (d, 1H).

2.3.2. Synthesis of 4-((4-ethynylphenyl)diazinyl)-*N*,*N*-dimethylaniline (Azo1, Scheme 2). A 10 mL aqueous solution of sodium nitrite (0.69 g, 6.03 mmol) was added dropwise to a 70 mL aqueous solution of 4′-dimethylaminophenyl acetylene (1.17 g, 10.00 mmol) acidified by concentrated hydrochloric acid (3.5 mL) at 0–5 °C. Separately, *N*,*N*-dimethylaniline (1.22 g, 10.00 mmol) and 10 g of sodium acetate were dissolved in 10 mL of water and cooled to 0 °C. Then, the diazotized solution was added slowly into the alkaline solution of *N*,*N*-dimethylaniline with continuous stirring in an ice bath. After the addition was complete, stirring was continued for 4 h. The precipitate was filtered and washed with water. The crude product was recrystallized from ethanol and dried by vacuum to generate bright red crystals (1.26 g, 55.80%). ^{1}H NMR (DMSO-d_6, ppm): $H_{4,3}$: 7.75–7.82 (m, 4H), H_2: 7.61 (d, 2H), H_5: 6.84 (d, 2H), H_1: 4.37 (s, 1H), H_6: 2.50 (s, 6H).

2.3.3. Synthesis of 4-((4-methoxyphenyl)diazenyl)phenol (Azo2, Scheme 3). A 10 mL aqueous solution of sodium nitrite (0.69 g, 0.010 mol) was added dropwise to a 10 mL aqueous solution of *p*-anisidine (1.23 g, 0.010 mol) acidified by concentrated hydrochloric acid (3.3 mL) at 0–5 °C. Separately, phenol (0.93 g, 0.010 mol) and sodium hydroxide (0.4 g, 0.010 mol) were dissolved in 5 mL of water and cooled to 0 °C. Then, the diazotized solution was added slowly into the alkaline solution of phenol with continuous stirring in an ice bath. After the addition was complete, stirring was continued for 4 h. The resulting mixture was acidified by 6 M hydrochloric acid and stirred for 30 min. The precipitate was filtered, washed with water and hexane, and dried by vacuum. The crude product was recrystallized from CH_2Cl_2/hexane to generate orange rod-shaped crystals (1.54 g, 67.70%). ^{1}H NMR (DMSO-d_6, ppm): H_1: 10.19 (s, 1H), H_3: 7.82 (d, 2H), H_4: 7.76 (d, 2H), H_5: 7.10 (d, 2H), H_2: 6.93 (d, 2H), H_6: 3.85 (s, 3H).

2.3.4. Synthesis of poly(ether sulfone)s with bromine groups (PES, Scheme 4). Potassium carbonate (0.84 g, 6.36 mmol) was added to 10 mL of *N*,*N*-dimethylacetamide (DMAc), 5 mL of toluene solution of 2-(4′-bromophenyl) hydroquinone (1.32 g, 5.00 mmol), and 4,4′-difluorodiphenyl sulfone (1.27 g, 5.00 mmol) at 135 °C for 4 hours to remove water generated during the reaction. The temperature was increased to 150 °C, and stirring was continued for 7 hours. The precipitate was slowly poured into water under stirring and washed with water and ethanol. The crude product was washed three times with water and ethanol to obtain a white powder (2.20 g, 91.70%).

2.3.5. Synthesis of Azo-PES-1 (Scheme 5). CuI (0.01 g, 0.06 mmol) and triethylamine (0.09 g, 0.084 mmol) were added to

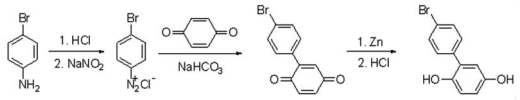

Scheme 1 Synthetic route of 2-(4′-bromophenyl) hydroquinone.

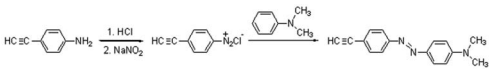

Scheme 2 Synthetic route of Azo1.

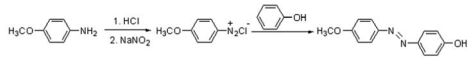

Scheme 3 Synthesis routes to Azo2.

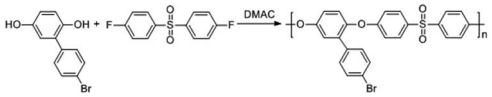

Scheme 4 Synthesis routes to Azo-CPAE-2.

a 10 mL of DMAC solution of PES (0.32 g), Azo1 (0.25 g, 1.00 mmol), and bis(-triphenylphosphine)dichloropalladium($Pd_2(Ph)_2Cl_2$) (0.03 g, 0.04 mmol). The mixture was degassed and filled with nitrogen and then heated at 100 °C under nitrogen for 12 h. After being slowly poured into aqueous HCl (200 mL, 1 mol), the precipitate was filtered, washed with water and ethanol, and dried by vacuum to generate orange powder (0.33 g, 66.7%). Found: C, 63.89; H, 3.52; N, 2.77.

2.3.6. Synthesis of Azo-PES-2 (Scheme 6). CuCl (0.01 g, 0.06 mmol) and Cs_2CO_3 (0.28 g, 0.88 mmol) were added to a 10 mL DMAc solution of PES 0.30 g, Azo2 (0.23 g, 1.00 mmol), and 2,2,6,6-tetramethylheptane-3,5-dione (TMHD) (0.15 g, 0.08 mmol). The mixture was degassed and filled with nitrogen and then heated at 100 °C under nitrogen for 12 h. After being slowly poured into aqueous HCl (200 mL, 1 mol), the precipitate was filtered, washed with water and ethanol, and dried by vacuum to generate orange powder (0.31 g, 71.4%). Found: C, 66.78; H, 3.80; N, 1.96.

3. Results and discussion

3.1. Synthesis and characterization

Compared with a branch chain polymer, a main chain polymer can be prepared by a simple polymerization method without bifunctional azobenzene, retaining the mechanical properties of the original polymer to the greatest extent. The maximum absorption peak wavelength of the ultraviolet-visible spectrum of methoxy group azobenzene and alkynyl azobenzene is long, and it can be isomerized under green light or red light. Therefore, the photoinduced deformation of polymers can be achieved under green or red light irradiation by introducing alkynyl azobenzene (Azo1) or methoxy azobenzene (Azo2). As shown in Fig. S1,† the stretching vibration absorption peak of the phenolic hydroxyl group was located at 3364 cm^{-1}. The ^1H NMR spectrum of the compound 2-(4′-bromophenyl) hydroquinone (Fig. S4†) showed that the proton peaks in the structure could be assigned accordingly, proving the synthesis of the compound 2-(4′-bromophenyl) hydroquinone. As shown in Fig. S5,† the single peak at 3.07 ppm referred to the methyl proton peak connected to the N atom in the structure. The single peak at 4.37 ppm denoted the hydrogen proton peak linked to the alkynyl group in the structure, which proves the synthesis of azobenzene derivative Azo1. As shown in Fig. S3,† there was a stretching vibration absorption peak of phenolic hydroxyl at 3417 cm^{-1}. As shown in Fig. S6,† the single peak at 3.85 ppm was ascribed to the proton peak of the hydrogen atom on the methoxy group in the structure, and the other proton peaks were assigned accordingly, proving that pure azobenzene derivative Azo2 had been synthesized. The results indicated that the small-molecule compounds involved in the reaction had been successfully synthesized.

In this paper, bromine-containing PES was synthesized, and then azobenzene derivatives (Azo1 and Azo2) were connected to the main chain through a substitution reaction to prepare azo-containing poly(aryl ether sulfone)s (Azo-PES-1 and Azo-PES-2). The synthesis route is shown in Schemes 5 and 6. The synthesis strategy not only retained the mechanical properties of the original poly(aryl ether sulfone)s, but also avoided the difficulties in the polymerization process caused by the complex monomers. In Table 1 it can be seen that all the polymers had number average molecular weights greater than 5.88×10^4 g mol^{-1}. The structures of the polymers were characterized by IR, ^1H NMR, and elemental analysis.

The infrared spectra of the three types of poly(aryl ether)s are shown in Fig. 1, with an absorption peak of aromatic ether bonds at 1240 cm^{-1}.[27] The absorption peak of 2920 cm^{-1} of Azo-

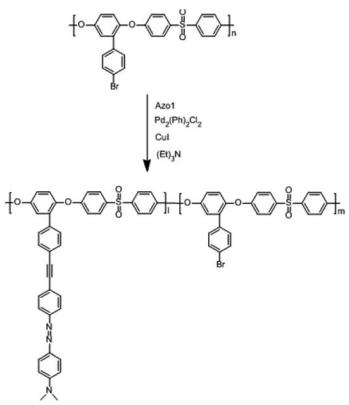

Scheme 5 Synthesis routes to Azo-PES-1.

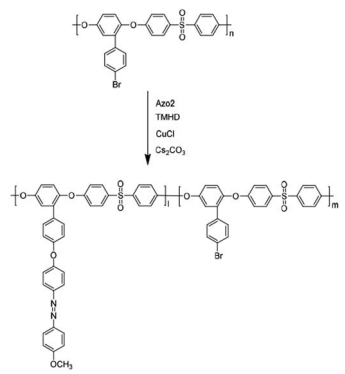

Scheme 6 Synthesis routes to Azo-PES-2.

Table 1 Properties of the polymers

Sample	M_n	M_w/M_n	T_g[a] (°C)	T_{d5}[b] (°C)	T_{d10}[c] (°C)
PES	5.88×10^4	2.0	200	321	379
Azo-PES-1	6.65×10^4	1.8	193	349	507
Azo-PES-2	6.54×10^4	2.1	185	349	467

[a] Glass transition temperature by DSC. [b] 5% weight-loss temperatures were detected at a heating rate of 10 °C min^{-1} in nitrogen. [c] 5% weight-loss temperatures were detected at a heating rate of 10 °C min^{-1} in nitrogen.

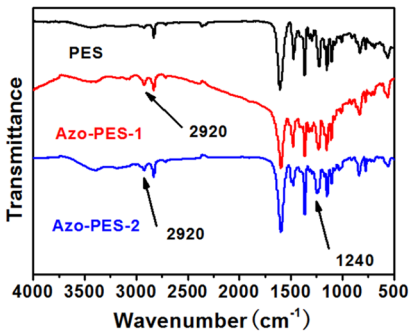

Fig. 1 FT-IR spectra of PES, Azo-PES-1, and Azo-PES-2.

PES-1 is the stretching vibration of the methyl group and the absorption peak of 2920 cm^{-1} of Azo-PES-2 is the stretching vibration of the methyl group. The infrared spectra of the three polymers showed similar absorption peaks, proving that the target polymer had been synthesized.

According to the elemental analysis results for the two polymers, the grafting rates (calculated based on N content) of Azo-PES-1 and Azo-PES-2 were 37% and 36%, respectively.

The ^{1}H NMR spectra of the three polymers in DMSO-d_6 are shown in Fig. 2. The chemical shift of hydrogen on the benzene ring of the polymers was difficult to distinguish due to their overlapping with each other. Compared to the ^{1}H NMR spectra of PES, new signals of proton a (the curve of Azo-PES-1) and proton b (the curve of Azo-PES-2) could be observed at 3.09 ppm and 3.84 ppm, respectively.

3.2. Photoinduced isomerization behavior of the polymers

The response speed to light is the fundamental factor in determining whether azobenzene-containing compounds can

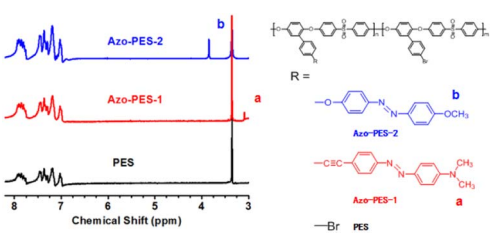

Fig. 2 ^{1}H NMR spectra of PES, Azo-PES-1, and Azo-PES-2.

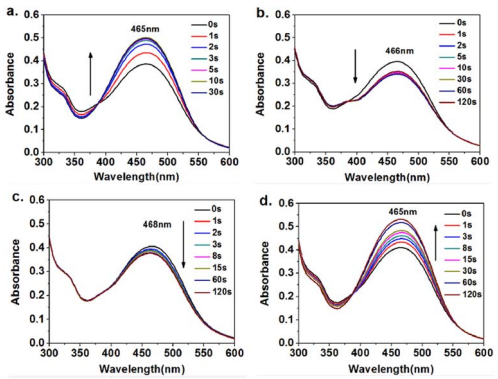

Fig. 3 Time-evolved absorption spectra of Azo-PES-1 upon irradiation at 365 nm (a), at 450 nm (b), at 532 nm (c), and at 660 nm (d) in DMF solution.

serve as photoinduced deformation materials. As shown in Fig. 3a, with the extension of UV irradiation time at 365 nm, the n–π* transition absorption peak of Azo-PES-1 at 465 nm gradually increased in the DMF solution. As the exposure time to 450 nm blue light was prolonged, the absorption peak of the n–π* transition at 466 nm weakened (Fig. 3b). As the green light illumination time at 532 nm was prolonged, the absorption peak of the n–π* transition at 468 nm weakened (Fig. 3c). With the extension of illumination time at 660 nm of red light, the n–π* transition absorption peak at 465 nm increased (Fig. 3d). Under different wavelengths of light, the UV-vis spectra all showed isosites at 387 nm, indicating that no chemical changes had occurred in the process of light irradiation except *cis–trans* isomerization of azobenzene. The intensity of the absorption peak of the n–π* transition at 465 nm increased under irradiation with ultraviolet light and red light and decreased under irradiation with blue light and green light, due to the isomerization of some azobenzene molecules under natural light irradiation during the preparation process of the compound solution. Therefore, the 365 nm and 660 nm light caused some azobenzene to transition from *trans*-to *cis*-, and the light at 450 nm and 532 nm caused the isomerization of some

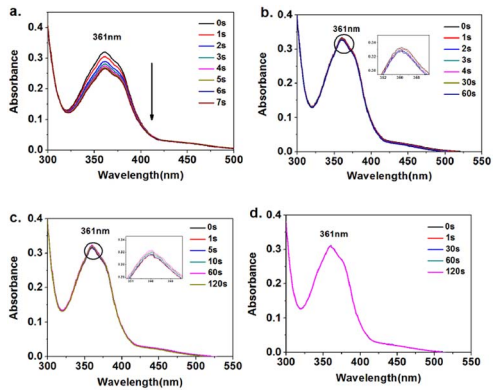

Fig. 4 Time-evolved absorption spectra of Azo-PES-2 upon irradiation at 365 nm (a), at 450 nm (b), at 532 nm (c), and at 660 nm (d) in DMF solutions (50 μM).

azobenzene from *cis*-to *trans*-. The UV-vis spectra of the polymer solutions at various wavelengths demonstrated that the polymers underwent photoinduced isomerization behavior with a high photoinduced isomerization rate, reaching photostability within a few seconds, providing important support for subsequent research into photoinduced deformation.

The photoinduced deformation behavior of the polymer solution at various wavelengths is shown in Fig. 4. Under 365 nm, 450 nm, and 532 nm light irradiation, the π–π* transition absorption peak at 361 nm of Azo-PES-2 in DMF solution weakened with the extension of light irradiation time. Although the intensity of the absorption peak changed less, the photoisomerization rate was faster, and photostability was achieved in a few seconds, indicating that some azobenzene molecules underwent isomerization. However, the π–π* transition absorption peak of Azo-PES-2 at 361 nm remained almost unchanged under irradiation with 660 nm red light, which proved that red light cannot cause the photoisomerization of azobenzene in Azo-PES-2.

The photoisomeric behavior of the polymers in the thin film state was investigated. The polymer solution was dropped onto a neat 1 cm × 5 cm transparent quartz sheet and dried to prepare a thin film with a thickness of approximately 1 μM. The UV background from the quartz film was subtracted and irradiated at 450 nm for different times before measuring the UV-visible spectrum of the film. As shown in Fig. 5, the maximum absorption peak positions of the UV visible spectra of the two polymer films were basically consistent with the UV spectra of the solution. Under 450 nm illumination, the UV visible spectra of both polymers were changed. Among them, the n–π* transition absorption peak at 452 nm in Azo-PES-1 decreased and reached photostability within 1 minute. The azobenzene group

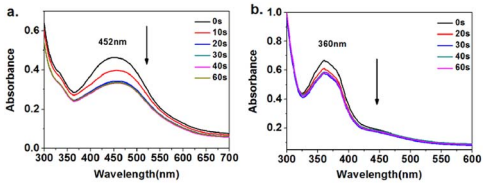

Fig. 5 Time-evolved absorption spectra of Azo-PES-1 film (a) and Azo-PES-2 film (b) upon irradiation by a 450 nm LED.

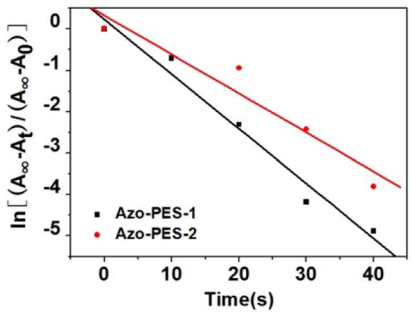

Fig. 6 The first-order *trans*-to-*cis* photoinduced isomerization kinetics of Azo-PES-1 and Azo-PES-2.

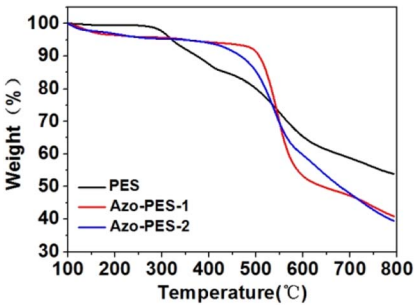

Fig. 7 TGA curves of Azo-PES-1 and Azo-PES-2.

was located in the side chain, and the *trans–cis* isomerization did not need to overcome the resistance caused by the movement of the main chain segment, and the molecular motion was relatively free. The reduction in the π–π* transition absorption peak and rapid isomerization of Azo-PES-2 at 360 nm confirmed the above conclusion.

The rate constants of *trans–cis* isomerization for each polymer were calculated using the following formula:

$$A_t = A_\infty + (A_0 - A_\infty)\exp(-kt)$$

A_t refers to the maximum absorption peak absorbance for different illumination times (t) under 450 nm light, A_∞ indicates the maximum absorption peak absorbance in the steady state under 450 nm illumination, and A_0 denotes the maximum absorption peak absorbance without illumination under 450 nm light.

The curve of $\ln[(A_\infty - A_t)/(A_\infty - A_0)]$ against irradiation time t is shown in Fig. 6. Several polymers exhibited a linear relationship between $\ln[(A_\infty - A_t)/(A_\infty - A_0)]$ and irradiation time, proving that the *trans–cis* isomerization behavior of the azobenzene polymers followed first-order reaction kinetics.[36–38] The photoisomerization rates of Azo-PES-1 and Azo-PES-2 azobenzene polymers under 450 nm LED light irradiation were calculated as 0.13 s^{-1} and 0.094 s^{-1}, respectively. The photoinduced isomerization rate of Azo-PES-1 was larger than that of Azo-PES-2, because the absorption wavelengths of Azo-PES-1 was more compatible with the excitation light than that of Azo-PES-2.

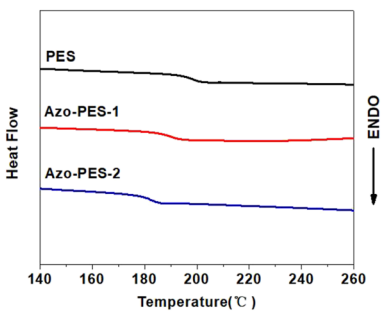

Fig. 8 DSC curves of Azo-PES-1 and Azo-PES-2.

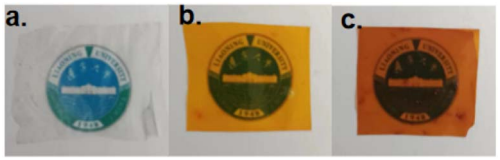

Fig. 9 The transparency of PES (a), Azo-PES-2 (b), and Azo-PES-2 (c) films.

3.3. Thermal properties of the polymers

A poly(aryl ether) is a kind of high-performance polymer with good thermal stability. The thermal stability of the three polymers was characterized using thermogravimetric analysis technology. As shown in Fig. 7, the temperatures at 5% and 10% thermal weight loss of all polymers were above 320 °C and 350 °C under an N_2 atmosphere, which indicated that the prepared polymers had good thermal stability.

The glass transition temperature of the polymer was measured using DSC under a nitrogen atmosphere, as shown in Fig. 8. The three polymers prepared possessed high glass transition temperatures, which were all above 180 °C, as listed in Table 1.

3.4. Photoinduced deformation behavior of the polymers

1.5 mL DMAc solutions of 0.07 g of PES, Azo-PES-1, and Azo-PES-2 were each heated to dissolve fully, and filtered with a filter cloth. The clarified polymer solution was dropped onto a horizontal glass plate (size: 25 mm × 75 mm) and dried at 50 °C for 2 h. Then, the polymers were gradually heated to 60 °C, 70 °C, 80 °C, and 100 °C for 1 h, respectively, to remove the bubbles in the polymer films. The glass sheet covered with polymer was soaked in distilled water, and then the films were separated from the glass sheet. The dry films were prepared for use. After removing the uneven areas around them, the films were obtained as shown in Fig. 9, with a thickness of about 20 μm. It can be seen that the films were uniform and transparent.

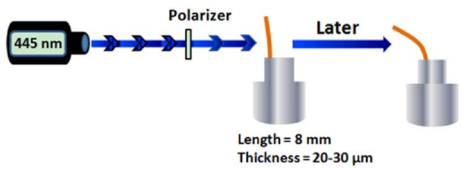

Fig. 10 The evolutionary process of the photoinduced deformation behavior of the cantilevers.

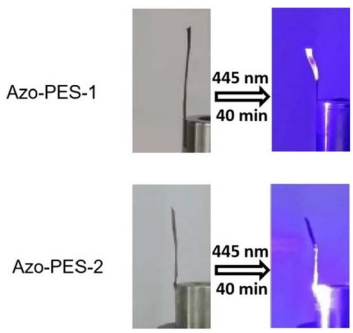

Fig. 11 The photoinduced deformation behavior of the cantilevers under irradiation by a 445 nm laser (100 mW cm^{-2}).

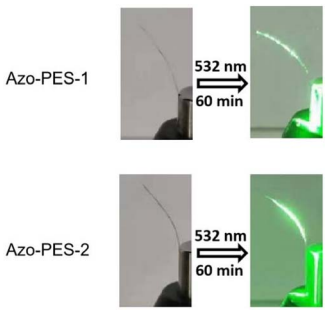

Fig. 12 The photoinduced deformation behavior of the cantilevers under irradiation by a 532 nm laser (100 mW cm^{-2}).

The testing process for photoinduced deformation of the cantilevers of the polymers was as follows: the cantilevers were cut to an 8 mm × 2 mm × 20 μm size.[39,40] The samples were irradiated by a 445 nm laser light source, in which the distance between the light source and the polarizer was 10 cm, and the distance between the polarizer and the sample cantilever was also 10 cm (Fig. 10). The photoinduced deformation properties of the cantilevers were measured under irradiation by 445 nm, 532 nm, and 660 nm lasers at room temperature, as shown in Fig. 11–13.

As shown in Fig. 11, the cantilevers of the polymers have bent towards the light (from 90° to 70°) after being illuminated by a 445 nm non-polarized laser for 40 min, which indicated that poly(aryl ether)s containing azobenzene groups in the side chain could undergo photoinduced deformation. Fig. 12 shows the photoinduced deformation behavior of the cantilevers of the polymers after being illuminated by a 532 nm non-polarized laser for 60 min. It can be seen that the cantilevers of the polymers could undergo photoinduced deformation (bending from 70° to 50°) after being illuminated by a 532 nm non-polarized laser for 60 min.

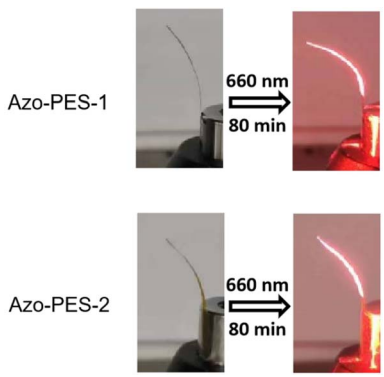

Fig. 13 The photoinduced deformation behavior of the cantilevers under irradiation by a 660 nm laser (100 mW cm^{-2}).

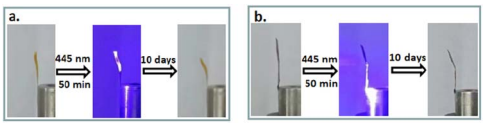

Fig. 14 The photoinduced deformation behavior and stability of cantilevers of Azo-PES-1 (a) and Azo-PES-2 (b) under irradiation by a 445 nm laser and after 10 days in the dark.

Fig. 13 shows the photoinduced deformation behavior of the cantilevers of the polymers after being illuminated by a 660 nm non-polarized laser for 80 min. After being illuminated by 532 nm non-polarized laser, it can be seen that the cantilever of Azo-PES-1 could undergo photoinduced deformation (bending from 65° to 45°), but the cantilever of Azo-PES-2 could not undergo photoinduced deformation. The reason was that Azo-PES-2 showed almost no absorption at 660 nm.

The stability of the photoinduced deformation behavior of the cantilevers of the polymers is shown in Fig. 14. No relaxation of either cantilever to its original position was found 10 days after irradiation. This proved that the two kinds of polymer cantilever show good photoinduced deformation stability.

4. Conclusions

In summary, two novel poly(aryl ether)s containing azobenzene groups in the side chain were synthesized. The elemental analysis data showed that the grafting rates of azobenzene were 37% and 36%, respectively. Their photoresponsive properties were studied. It could be seen that both polymers could undergo photoinduced deformation under a 445 nm laser and a 532 nm laser. Azo-PES-1 could undergo photoinduced deformation under a 660 nm laser, but Azo-PES-2 could not undergo photoinduced deformation under a 660 nm laser. It could be seen that the excitation luminescence match to the maximum absorption peak of the azobenzene groups was more compatible, and the photoinduced motion of the polymers was faster. In addition, poly(aryl ether)s containing azobenzene groups in the side chain showed good photoinduced deformation stability (over 10 days). The results of this work are helpful for designing polymers which could be controlled by lasers with different wavelengths.

Conflicts of interest

There are no conflicts to declare.

Acknowledgements

The authors gratefully acknowledge the National Natural Science Foundation of China (Grant No. 51703089) and the Basic Research Projects of Higher Education Institutions of Liaoning Provincial Department of Education (Grant No. LJKFZ20220175) for financial support.

References

1 A. Kirillova and L. Ionov, *J. Mater. Chem. B*, 2019, **7**, 1597–1624.
2 K. Oliver, A. Seddon and R. S. Trask, *J. Mater. Sci.*, 2016, **51**, 10663–10689.
3 M. Behl, M. Y. Razzaq and A. Lendlein, *Adv. Mater.*, 2010, **22**, 3388–3410.
4 Y. M. Wang, Y. N. Wang, Q. H. Wei and J. Zhang, *Eur. Polym. J.*, 2022, **137**, 111314.
5 J. Y. Kim, S. W. Kang, S. H. Kim, B. C. Kim, K. B. Shim and J. G. Lee, *Macromol. Res.*, 2005, **13**, 19–25.
6 T. Zheng and J. G. Wu, *Mater. Horiz.*, 2020, **7**, 3011–3020.
7 J. M. Gou, T. Y. Ma, R. H. Qiao, T. Z. Yang, F. Liu and X. B. Ren, *Acta Mater.*, 2021, **206**, 116631.
8 X. J. Liu, H. Q. Li, B. Y. Zhang, Y. J. Wang, X. Y. Ren, S. Guan and G. H. Gao, *RSC Adv.*, 2016, **6**, 4850–4857.
9 S. J. Jeon, A. W. Hauser and R. C. Hayward, *Acc. Chem. Res.*, 2017, **50**, 161.
10 F. X. Sun and D. S. Wang, *J. Mater. Chem. C*, 2022, **10**, 13700–13716.
11 T. Miyata, T. Namera, Y. L. Liu, A. Kawamura and T. Yamaoka, *J. Mater. Chem. C. B*, 2022, **10**, 2637–2648.
12 D. Habault, H. J. Zhang and Y. Zhao, *Chem. Soc. Rev.*, 2013, **42**, 7244–7256.
13 D. R. Wang and X. G. Wang, *Prog. Polym. Sci.*, 2013, **38**, 271–301.
14 A. Natansohn and P. Rochon, *Chem. Rev.*, 2002, **102**, 4139–4175.
15 O. Sakhno, L. M. Goldenberg, M. Wegener, C. Dreyer, A. Berdin and J. Stumpe, *Opt. Mater.*, 2022, **128**, 112457.
16 X. H. Lv, H. Y. Yan, Z. B. Wang, J. R. Dong, C. Liu, Y. Zhou and H. X. Chen, *Opt. Mater.*, 2023, **139**, 113755.
17 X. Y. Pan, Z. X. Zhu and Y. N. He, *Opt. Mater.*, 2023, **135**, 113324.
18 N. J. Li, J. M. Lu, H. Li and E. T. Kang, *Dyes Pigm.*, 2011, **80**, 18–24.
19 T. J. White, *J. Polym. Sci., Part B: Polym. Phys.*, 2018, **56**, 695–705.
20 T. J. White and D. J. Broer, *Nat. Mater.*, 2015, **14**, 1087–1098.
21 C. H. Zhang, X. G. Zhao, D. M. Chao, X. F. Lu, C. H. Chen, C. Wang and W. J. Zhang, *J. Appl. Polym. Sci.*, 2009, **113**, 1330–1334.
22 S. Georgi and K. A. I. Leonid, *Adv. Opt. Mater.*, 2019, 1900067.
23 D. H. Wan, K. M. Lee, Z. Yu, H. Koerner, R. A. Vaia, T. J. White and L. S. Tan, *Macromolecules*, 2011, **44**, 3840–3946.
24 R. C. Lan, J. Sun, C. Shen, R. Huang, Z. P. Zhang, C. Ma, J. Y. Bao, L. Y. Zhang, L. Wang, D. K. Yang and H. Yang, *Adv. Funct. Mater.*, 2020, **30**, 2000252.
25 T. Ube, K. Kawasaki and T. Ikeda, *Adv. Mater.*, 2016, **28**, 8212–8217.
26 T. Ikeda, J. Mamiya and Y. L. Yu, *Angew. Chem., Int. Ed.*, 2007, **46**, 506–528.
27 M. L. Baczkowski, D. H. Wang, D. H. Lee, K. M. Lee, M. L. SmithL, T. J. White and L. S. Tan, *ACS Macro Lett.*, 2017, **6**(12), 1432–1437.

28 X. J. Sun, J. Wei and Y. L. Yu, *Polym. Chem.*, 2022, **13**, 5447–5452.
29 J. J. Wie, D. H. Wang, K. M. Lee, T. J. White and L. S. Tan, *J. Mater. Chem. C*, 2018, **6**, 5964–5974.
30 Y. X. Zhang, J. H. Yuan, X. Zhao, L. Wu, Z. Liu and X. M. Song, *Polym. Chem.*, 2022, **13**, 569–576.
31 Y. X. Zhang, X. F. Sun, X. L. An, *et al.*, *Dyes Pigm.*, 2021, **186**, 109018.
32 Y. X. Zhang, X. Zhao, J. H. Yuan, X. L. An, X. F. Sun, J. Yi and X. M. Song, *J. Mater. Chem. C*, 2021, **9**, 14139–14145.
33 K. S. Anna, S. B. Eva, S. Dariusz and K. Jolanta, *J. Mater. Chem. C*, 2019, **7**, 4032–4037.
34 Y. X. Zhang, S. Wang, Z. H. Wang, S. S. Gai and X. M. Song, *Des. Monomers Polym.*, 2017, **20**, 496–504.
35 Y. X. Zhang and S. Y. Chen, *RSC Adv.*, 2018, **8**, 37348–37355.
36 G. S. Kumar and D. C. Neckers, *Chem. Rev.*, 1989, **89**, 1915–1925.
37 X. Q. Xue, W. Zhang, Z. P. Chen, J. Zhu and X. L. Zhu, *J. Polym. Sci., Part A: Polym. Chem.*, 2008, **46**, 5626–5637.
38 Y. J. Yang YJ, S. Huang, Y. D. Ma, J. Yi, Y. C. Jiang, X. H. Chang and Q. Li, *ACS Appl. Mater. Interfaces*, 2022, **31**, 35623–35634.
39 P. P. Zhang, Z. X. Lan, J. Wei and Y. L. Yu, *ACS Macro Lett.*, 2021, **10**, 469–475.
40 D. H. Wang, K. M. Lee, D. H. Lee, M. Baczkowskiet, H. Park, M. E. McConney and L. S. Tan, *ACS Macro Lett.*, 2021, **10**, 278–283.